

## Grazing-Incidence Metal Mirrors for Laser-IFE

**M. S. Tillack, J. F. Latkowski\*, J. E. Pulsifer,  
K. L. Sequoia and R. P. Abbott\***

**September 2005**

\*Lawrence Livermore National Laboratory



## Grazing-Incidence Metal Mirrors for Laser-IFE

M. S. Tillack<sup>1</sup>, J. F. Latkowski<sup>2</sup>, J. E. Pulsifer<sup>1</sup>, K. L. Sequoia<sup>1</sup> and R. P. Abbott<sup>2</sup>

<sup>1</sup>University of California San Diego, La Jolla CA, USA

<sup>2</sup>Lawrence Livermore National Laboratory, Livermore CA, USA

*e-mail contact of main author: mtillack@ucsd.edu*

The final optic in a laser-IFE power plant beamline experiences direct line-of-sight exposure to target emissions, including neutrons, x-rays, high-energy ions and debris. It must withstand this environment reliably over many months of continuous operation, while simultaneously meeting stringent optical requirements. A grazing-incidence metal mirror has been considered as a potentially robust design option that can survive acceptably high laser fluence as well as the harsh environment of an inertial fusion reactor chamber. We have explored the design options and responses of metal mirrors in a coordinated program of modeling, mirror fabrication and experiments. Our results indicate that grazing-incidence metal mirrors have the ability to survive the IFE environment while satisfying the requirements on beam quality necessary for successful target implosion.

### 1. Introduction

The final optic in a laser-IFE power plant necessarily is exposed directly to target emissions and the chamber environment. The minimum requirement on this optic is to deflect the beam so that the remaining optics are protected against these threats. Other optical functions such as focusing, steering or wavefront correction can be performed upstream of the final optic.

**Fig. 1** shows a design concept that places the final optic a distance of 20-30 m from the chamber center, such that the threats are reduced by an order of magnitude or more as compared with the chamber wall. This separation also provides an opportunity to mitigate the threats due to energetic ions and contaminants.

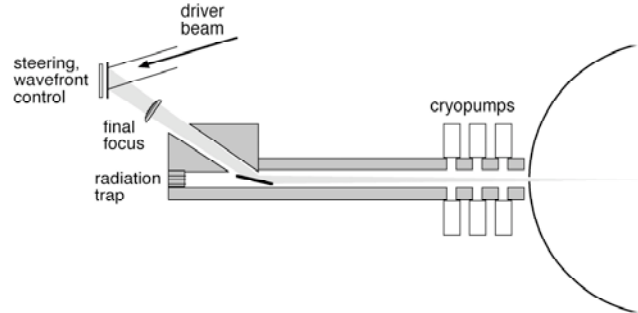


*Fig. 1 Schematic layout of a power plant beamline*

A grazing-incidence metal mirror (GIMM) was chosen primarily due to concerns over radiation damage to dielectric materials [1]. However, the reflectivity of metal mirrors, especially in the UV part of the spectrum, is much lower than that of multi-layer dielectrics. To overcome this limitation, we chose to concentrate our efforts on Al, which retains its reflectivity below 248 nm, which is the shortest wavelength currently considered for IFE. In addition, the use of s-polarized light at a shallow angle ( $\sim 85^\circ$ ) allows us to increase the reflectivity above 99% (see Fig. 2). This Al reflector most likely will be placed on a substrate which is optimized to maintain good surface figure over the lifetime of the optic.

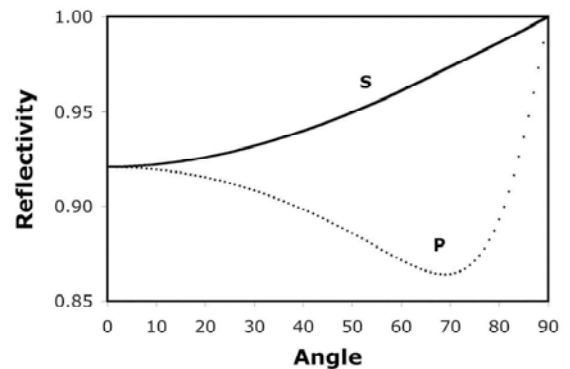


*Fig. 2 Reflectivity of s- and p-polarized light on pure Al at 248 nm*

Requirements on the final optic have been developed as a part of the High Average Power Laser (HAPL) program [2]. HAPL is a coordinated, focussed multi-lab effort to develop the science and technology for Laser Inertial Fusion Energy based on direct drive targets and solid chamber walls. The requirements are listed in Table I together with nominal values of the threats.

Laser-induced damage is primarily thermo-mechanical in nature. In a grazing angle configuration, the basic stability is in question, because defects which expose the surface to a higher angle of incidence will lead to higher absorption than the pristine surface. By controlling the microstructure of the surface and optimizing the interface between the reflector and substrate, we have demonstrated high damage threshold (above  $10 \text{ J/cm}^2$ ) with shot counts up to  $10^5$ .

Radiation damage can cause physical, mechanical and optical changes to the mirror. This includes gross macroscopic swelling, surface roughening, and thermomechanical changes similar to laser-induced damage. We have examined the threat spectrum at the mirror location, explored the damage mechanisms and initiated an experimental program using neutron, ion and x-ray sources.

## 2. Fabrication and Laser Damage Testing

Several fabrication techniques have been explored in order to develop a mirror with acceptable optical quality as well as high laser-induced damage threshold. We have created mirrors by bonding foils to substrates, thin film deposition, electroplating, diamond-turning, polishing, and various combinations of these (see Fig. 3). Test articles were exposed with a Lambda Physik Compex 201 excimer laser using a KrF gas mixture producing 248-nm light with a pulse length of approximately 25 ns. The beam was polarized and attenuated using cube beamsplitters, focused on the specimens with a 15-20 cm focal length lens in order to increase the fluence, and finally reflected from the specimen at an angle of incidence 85 degrees from the surface normal (see Fig. 4). The nominal test fluence used for experiments was  $5 \text{ J/cm}^2$  for the majority of tests, as measured perpendicular to the propagation direction (**not** relative to the surface), with some samples exposed to as much as  $50 \text{ J/cm}^2$ . The beam footprint on target is trapezoidal with an area approximately  $1 \times 3 \text{ mm}^2$ . Early testing was performed in air, but chemical reactions quickly forced us to perform all tests in a clean, oil-free vacuum produced by a cryopump.

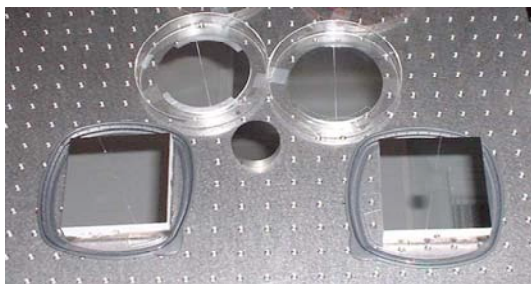


Fig. 3 Photograph of 10-cm test mirrors

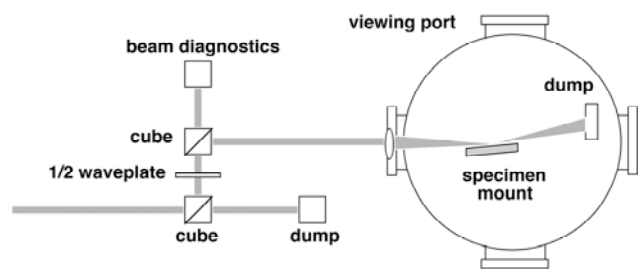


Fig. 4 Experimental setup

TABLE I: PERFORMANCE GOALS AND REQUIREMENTS ON THE FINAL OPTIC

Metric	Value
Minimum lifetime	$3 \times 10^8$ shots
Surface figure	80 nm ( $\lambda/3@248 \text{ nm}$ )
RMS roughness	<5 nm
Scattering	<1%
Waste disposal rating	Class C
Laser fluence (normal to beam)	$5 \text{ J/cm}^2$
X-ray fluence per shot	$20\text{-}80 \text{ mJ/cm}^2$
Average x-ray energy	3-4 keV
Ion fluence per shot (unattenuated)	$0.4\text{-}1.1 \text{ J/cm}^2$
14-MeV neutron flux	$5 \times 10^{12} \text{ n/cm}^2\text{-s}$
Total neutron flux	$10^{13} \text{ n/cm}^2\text{-s}$

A standard test procedure was developed in order to clean and condition optics in the chamber. Tests began when the chamber pressure dropped below  $10^{-4}$  Torr. The beam was initially attenuated with a 1/2-waveplate and polarizing cube in order to gradually increase the fluence while surface contaminants were dislodged and some mechanical shakedown occurred. Samples were exposed for 100 shots at 1 Hz and several gradually increasing energy levels. Although the laser operates well into the UV part of the spectrum, observation of visible changes was one of the most valuable in-stu diagnostics. Most aluminum surfaces tested normally exhibit some amount of mild (blue) fluorescence. Bright fluorescence, however, is usually an indication of an imperfect surface finish, contamination on the surface, or damage initiation.

### 2.1 Monolithic Polycrystalline Aluminum

In the early stages of laser damage studies, we observed that absorptive particles in aluminum alloys, such as Al-1100 and Al-6061, cause damage at relatively low fluence. Therefore, all of our test samples used high purity Al (typically 99.999%). Initially, rolled sheets with 1-mm thickness were cut and bonded to Al alloy substrates using cyanoacrylate glue. The grain size for these sheets was of the order of 100  $\mu\text{m}$ . These mirrors were given a mirror quality surface by either mechanical polishing or diamond turning.

In the mechanical polishing process, the surface finish was achieved using polishing wheels with a series of 5, 1, and 0.04  $\mu\text{m}$  alumina polishing suspension. Wyko optical profiling indicates an average RMS surface roughness ranging from 30 to 45 nm. During testing, the fluence was ramped up to a maximum value of 5  $\text{J}/\text{cm}^2$  using 10 shots per fluence level during the cleaning phase. After these 50 shots, damage was already visible. Figs. 5 and 6 clearly show the presence of grain motion and slip line transport within grains. Accumulated plastic deformation is the dominant limitation on the lifetime of large-grained surfaces.

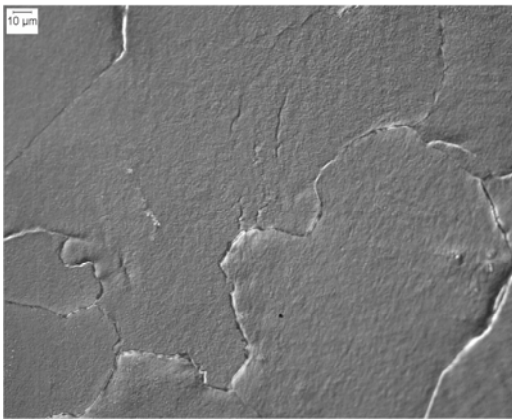


Fig. 5 Optical micrograph of Al foil showing grain boundary separation after 50 shots

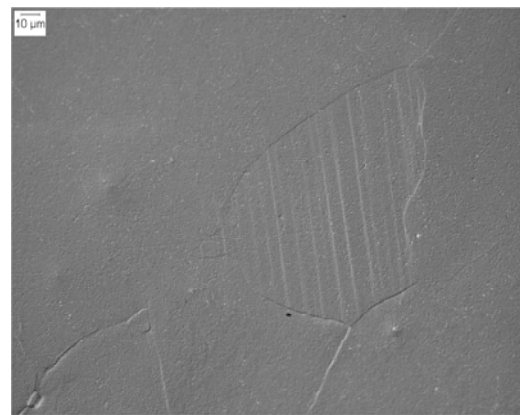


Fig. 6 Optical micrograph of Al foil showing slip lines within grains after 50 shots

Diamond turning is a procedure which uses a high precision lathe to produce a flat and smooth surface. Fig. 7 shows the surface of one of the Al mirrors prepared at the General Atomics micro-machining laboratory. Wyko optical profiling indicates an average RMS surface roughness ranging from 5.5 nm to 28 nm. Diamond turned surfaces typically do not have the high peaks like polished surfaces. Instead the surface contains periodic turning lines a few nanometers in height.

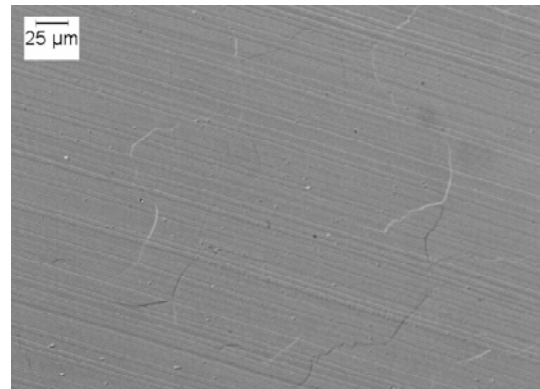


Fig.7 Optical microscopy of an unexposed diamond turned Al mirror

Figs. 8 and 9 show the morphology changes to these samples which were exposed to 450 pulses with a fluence range of 7 to 20  $\text{J}/\text{cm}^2$ . No damage was visible to the naked eye, but fluorescing began to occur, and continued to grow with time.

Diamond-turned mirrors survive longer than polished mirrors; perhaps the effects of turning help to stabilize the microstructure, or the effect of mechanical polishing exacerbates defects at grain boundaries. However, eventually diamond-turned mirrors suffer the same fate. Fig. 8 shows the two types of damage which are accumulating. Grain boundary decoration and separation are evident. In addition, small defects appear in the lower righthand part of the image. In Fig. 9, these “pits” are clearly the result of the erosion (etching) of the surface peaks created by diamond-turning. The laser appears to be trying to flatten the surface.

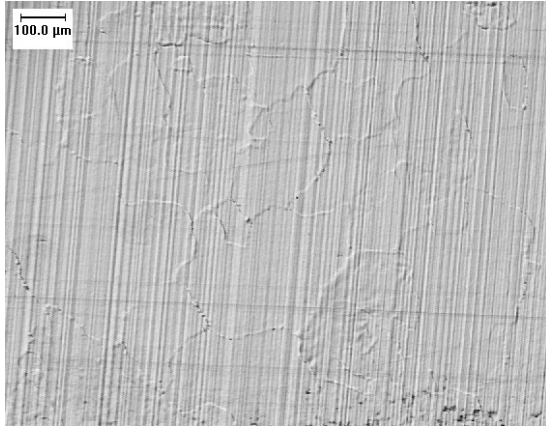


Fig. 8 Optical microscopy showing grain boundary decoration and distortion

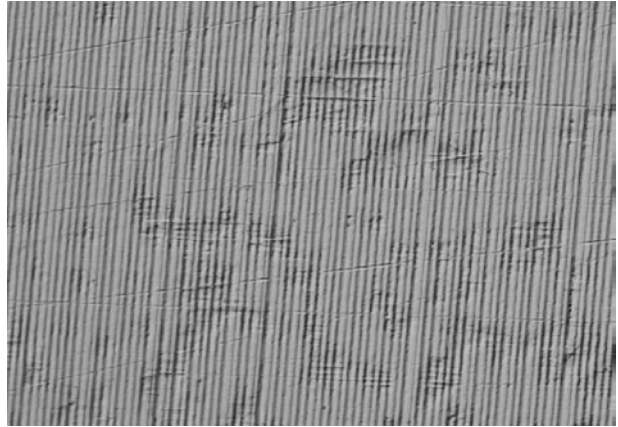


Fig. 9 Optical microscopy showing the UV etching of diamond lines

## 2.2 Thin Film Deposition on Polished Substrates

Sputter coating and e-beam evaporation have been used to produce thin film coatings of Al on various polished substrates. These coatings range in thickness from 100 nm up to several microns. The advantage of thin films is that they are nearly grain-free, which should make them more robust against high-cycle plastic deformations.

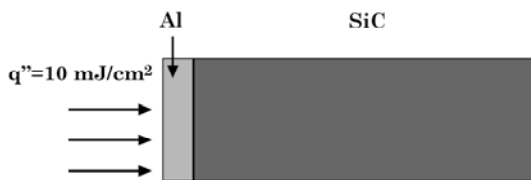
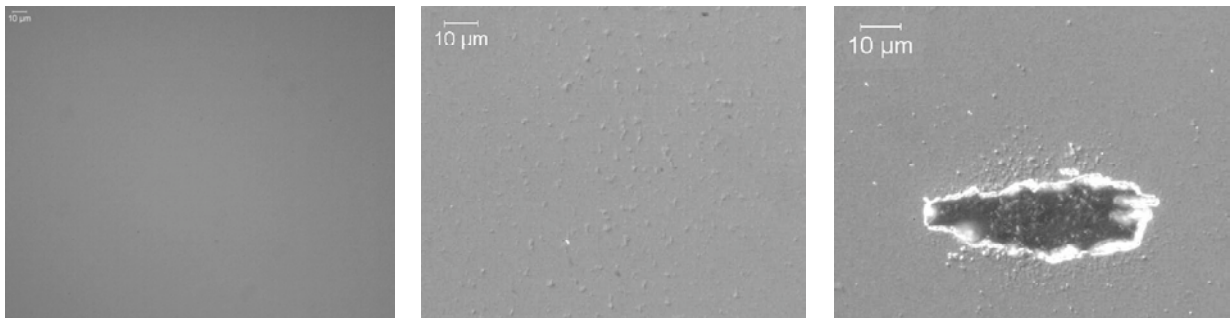


Fig. 10 Interface between the coating and substrate

The interface between a thin Al coating and its substrate is a major concern with thin films, which are not normally used in high fluence applications. This interface experiences a large thermomechanical stress due to the different thermal expansions of Al and the substrate (see Fig. 10). The stress field can cause small defects at the interface to grow, and in the worst case debond the coating from the substrate.

We have explored three potential solutions to overcome this problem: (1) strengthen the bond, (2) thicken the coating beyond the point where heat can diffuse to the interface during the pulse ( $\sim 5 \mu\text{m}$ ), and (3) reduce differential expansion by making the substrate from an Al alloy. In order to test bond integrity, we obtained superpolished CVD SiC optical flats from Rohm & Haas Corporation. These were coated by sputtering or e-beam evaporation. Fig. 11 shows a typical result (in this case with a 200 nm coating). The initially high-quality surface eventually exhibited small “pin-point” defects which we believe are initiated at microscopic defects at the interface. Eventually, these defects grow until they become absorptive (when the scale length is approximately equal to the wavelength of light). Catastrophic damage results when these thin films become damaged.



(a)

Fig. 11 Optical microscopy of 200 nm Al thin film showing (a) the initial condition, (b) incipient damage and (c) failure after 5000 shots at  $4 \text{ J/cm}^2$

A variety of other substrate processing techniques have been explored, including the use of a porous SiC slurry and a CVD Si overcoat on SiC/SiC; however we have not found any of these techniques to be capable of overcoming the fundamental problem of high interfacial stresses when the coating thickness is less than  $\sim 5 \mu\text{m}$ .

Films as thick as  $12 \mu\text{m}$  have been created by e-beam evaporation at Schafer Corp. Thicker films tend to survive higher fluences. For example, mirrors with coating thickness between  $2\text{-}5 \mu\text{m}$  have survived  $10^5$  shots up to  $5 \text{ J/cm}^2$ . Above about  $5 \mu\text{m}$ , the surface appearance becomes “milky” and the reflectivity degrades. At these thicknesses, grain growth can not be avoided. In order to regain the optical quality of e-beam coatings above  $5 \mu\text{m}$ , the surface can be repolished using diamond-turning or some other form of final finishing. Research on this multi-step fabrication procedure is ongoing.

### 2.3 Electroplating

In the electroplating process, a voltage is used to transport particles of the plating material from an anode to the object being plated within an acidic bath. This coating method yields relatively thick coatings, typically around a few hundred microns, with a measured grain size of the order of  $10 \mu\text{m}$ . Alumiplate Inc. produced several mirrors using Al-6061 as the substrate and a Ni strike layer for improved adhesion. After the substrates were coated, each was diamond turned at various machining facilities. An example surface micrograph is shown in Fig. 12.

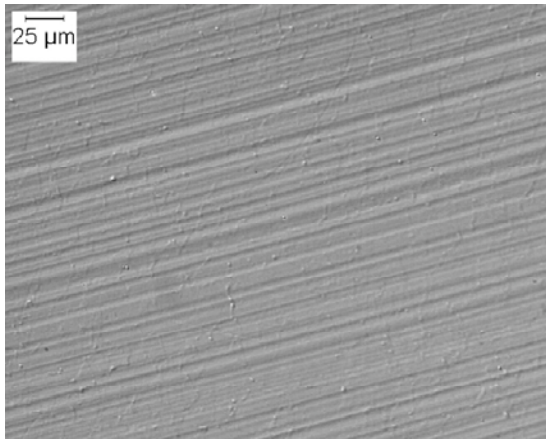


Fig.12 Optical microscopy of diamond turned electroplated mirror as fabricated

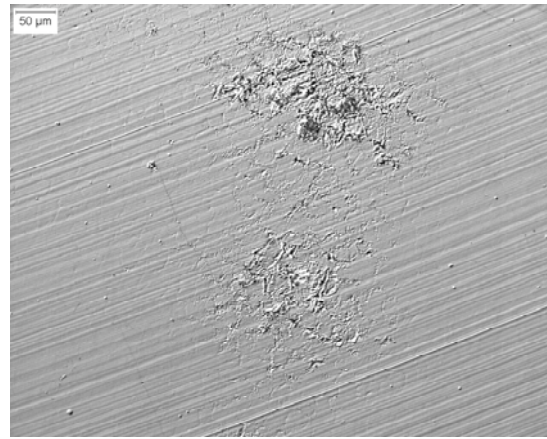


Fig. 13 Electroplated mirror showing damage after 95,000 shots at  $\sim 18 \text{ J/cm}^2$

The smaller grain size of the electroplating process appears to strengthen the surface and provide a higher damage threshold. This surface provided our best results to date, with a damage threshold of  $18 \text{ J/cm}^2$  at  $10^5$  shots. As seen in Fig. 13, eventually this surface too can be pushed to failure. Similar to the large-grain Al mirrors, damage initiates at grain boundaries and eventually becomes catastrophic when the defect height becomes comparable to the wavelength of light. For these samples, slip line transport was not observed. Fig. 14 shows data collected from several tests on electroplated mirrors at different fluences and shot counts. More data is needed to extrapolate into the elastic (high cycle) part of the curve.

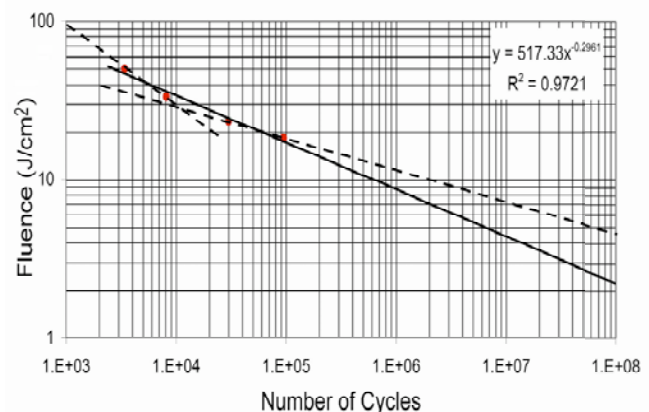


Fig. 14 Electroplated mirror fatigue curve

## 2.4 Alternative processing techniques and reflectors

Pure aluminum has a very low yield point (approximately 15 MPa). Our research indicates that control over the grain size can help extend the lifetime, but another potentially successful strategy would be to increase the yield strength by the controlled addition of a second element, such as Cu, Li, or Si. Solid solution hardening or nano-precipitate growth have been considered for improving the lifetime of our mirrors. If the precipitates are much smaller than the wavelength of light, then there is evidence that improvement in mechanical properties can be obtained without degradation of the optical quality. Research on these concepts is ongoing.

## 3. Radiation Damage and Mitigation

### 3.1 Radiation damage

Radiation damage may occur due to exposure to x-rays, ions or neutrons. X-ray damage is expected to be largely thermomechanical in nature. The XAPPER x-ray damage experiment is being used to confirm this expectation. XAPPER is based upon a pinch-based source developed and manufactured by PLEX LLC. Using an ellipsoidal condensing optic, XAPPER is capable of delivering x-ray fluences of 3-4 J/cm<sup>2</sup> in a 40 ns pulse. The source operates at up to 10 Hz and can deliver millions of pulses at a time. Additional details regarding the x-ray source and the XAPPER experiment can be found in references [3] and [4], respectively.

To date, XAPPER experiments have focused mainly on the effects of multi-pulse exposures of tungsten at relatively high x-ray fluences. Additional experiments have used aluminum mirrors, but also at fluences that far exceed those expected at the final optic. These experiments produce noticeable damage with only a single pulse. The challenge for upcoming experiments is to sufficiently and predictably reduce the x-ray fluence through a combination of defocusing the ellipsoidal optic and filtering both before and after the optic. Once this is accomplished, a series of experiments will be conducted. Analysis will include reflectivity and surface roughness measurements.

Ion damage experiments are beginning at Lawrence Livermore National Laboratory (LLNL) at the Ion Beam Laboratory (IBL). The IBL is able to provide ion fluences as high as 10<sup>18</sup> cm<sup>-2</sup> of ions ranging from H<sup>+</sup> to Xe<sup>+</sup> with ion energies from 2 keV to 20 MeV. Samples as large as 24" can be accommodated, and day-long runs are possible. The first IFE-relevant optics exposures will use 3 MeV He<sup>+</sup> ions exposed at a grazing angle of approximately 80 degrees. Exposure durations of 1-2 hours will provide ion fluences equivalent to several hours of exposure in an IFE system. Following these initial experiments, longer exposures are planned. The intent of the first round of experiments is to establish a lower limit at which significant optical damage is observed. Next, we will move on to higher levels of exposure to search for damage growth, saturation, and other effects. The data from these experiments is used to determine the degree to which methods of damage mitigation are to be implemented.

Low dose neutron irradiation has been completed for aluminum and multi-layer mirrors at Oak Ridge National Laboratory's High Flux Isotope Reactor (HFIR). Samples have been irradiated to fluences ranging from 1-5 × 10<sup>18</sup> n/cm<sup>2</sup>, which is roughly equivalent to 1.4-7 days of exposure in an IFE power plant. The low-fluence samples have been returned to LLNL and are currently being tested. The high-fluence samples are still at ORNL waiting for sufficient radioactive decay for handling and shipping. Analysis will include reflectivity measurements as well as cross-sectional transmission electron microscopy.

### 3.2 Damage Mitigation

The final optics in laser inertial fusion power plants will be exposed to ion radiation emanating from fusion targets. In earlier designs, the chamber was filled with xenon gas to a pressure of 500 mTorr [5]. This background gas absorbed the ions and re-radiated their energy as x-rays over a longer period of time. Unfortunately, calculations to determine target heating during injection suggest a xenon pressure limit between 10 and 50 mTorr. Additionally, updated target

output simulations show ion spectra considerably more energetic than those assumed in previous work. Calculations with SRIM [6] show that a significant fraction of the ions will impact the final optics causing damage through mechanisms including atomic displacements and bubble formation and growth.

To mitigate this threat to the final optics, a simple method was devised to deflect ions into robust beam tube walls using magnetic fields. Fig. 15 illustrates this concept. Shown schematically is the fusion chamber, a single beam tube with a final optic, and a Helmholtz coil pair to produce a magnetic field.

Three possible ion paths are depicted. The first is that of an ion that stops in the background gas because it possesses insufficient energy to penetrate to the final optic. The second is that of an ion of such high energy that it not only traverses the gas, but manages to cross the magnetic field and impact the optic. The third trajectory is the one that this scheme is attempting to maximize. Here, the ion is affected by the field enough to turn it into the beam tube wall and avoid a collision with the optic.

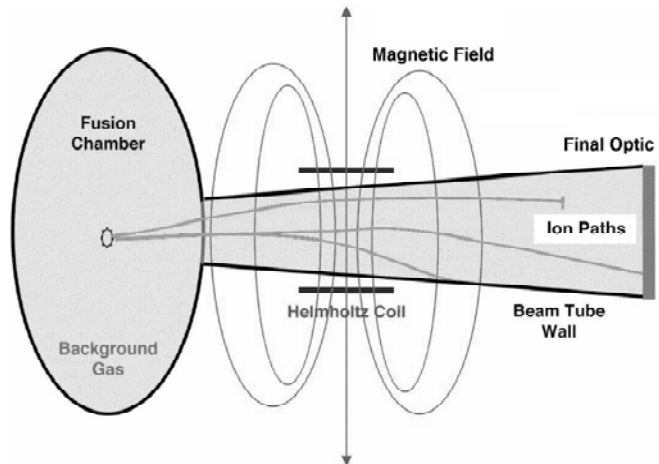


Fig. 15 Schematic representation of the ion mitigation concept

The DEFLECTOR code was written to determine what fraction of ions could be deflected away from final optics for a given magnetic field strength and location. It reads in target ion spectra [7], beam tube geometry, magnetic field strength and profile data, and appropriate stopping tables calculated with SRIM. Representative particles for each energy group are given an initially isotropic direction distribution and then transported through the chamber to interact with both the background gas and magnetic field. The impact time, position, energy, and angle are determined for each simulation particle that does not stop in the xenon. Fig. 16 shows a comparison of results for a simulation with no field and a simulation using a 0.1 T field.

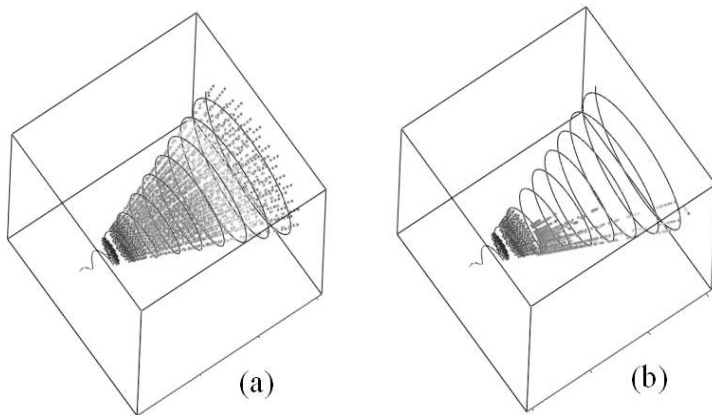


Fig. 16 Ion stopping and impact positions for all target output ions with (a) no magnetic field present and (b) a 0.1 T field (at center of coil pair) 9.0 m from chamber center. The scales are distorted with the perpendicular dimension expanded by 10x. The beam tubes extend 20 m from chamber center and have a diameter of  $\sim 1$  m at that point.

Deflector has shown that field strengths of 0.125 T can reduce ion energy fluence at 20 m by a factor of 40,000. Fields with higher strengths are capable of deflecting all ions. Since current designs call for final optic placement at 30 m or greater, it is reasonable to conclude that magnetic fields are a viable option for deflecting ions, thereby preventing ion damage to optics. Normal conducting magnets can be employed to generate the field strengths of interest (0.1–0.15 T). The power requirements for 60 Helmholtz coil pairs will range from 10 - 20 MW.



#### 4. Summary and Conclusions

We have shown that a grazing incidence metal mirror is a credible option for the final optic in a laser-driven IFE power plant. Mirrors have been fabricated up to 10 cm in diameter using technologies that scale to a full-size power plant optic. Testing and analysis have demonstrated thermomechanical resistance to laser-induced damage up to  $10^5$  shots using 248-nm light from a short-pulse KrF laser.

Damage resistance is improved by controlling the microstructure, especially the grain size, and by avoiding high thermal stresses at the interface between the reflector and substrate. Thin films thicker than 2 microns appear to survive  $10^5$  shots at the design fluence ( $5 \text{ J/cm}^2$ ) if the substrate is highly polished, but these coatings are inherently fragile. Very thick films (achieved with electroplating or thick PVD coatings) combined with a post-processing step to provide optical quality appear to be the most robust design choice. End-of-life exposures of mirrors are still needed in order to fully demonstrate these concepts.

High energy ions are a serious threat to the long-term survival of final optics. Even though the stand-off distance from the target emissions can be as high as 20-30 m, low chamber gas density requirements imposed by direct-drive cryogenic target injection prevents sufficient gas to protect against ions. We have shown that relatively modest magnetic fields provided around laser beamlines can divert more than 99.99% of the ions, such that we believe this threat can be mitigated. In addition, ion damage studies are underway using a steady-state particle accelerator in order to place an upper limit on the tolerable flux and energy of ions at the mirror.

Neutron damage is expected to be less problematic for metal mirrors as compared with multi-layer dielectric mirrors; however, testing is required in order to demonstrate this. High-fluence neutron exposure is a difficult challenge for all solid-state materials used in fusion energy devices, and will probably require construction of a neutron source before this issue can be resolved.

#### Acknowledgements

The authors wish to thank Ed Hsieh (Schafer Corp), Witold Kowbel (MER Corp), Jim Kaae, (General Atomics Corp), Gus Vallejo (Alumiplate Inc) and the members of the HAPL Team for fabrication support and valuable technical advice.

Financial support for this work was provided in part by the Naval Research Laboratory under contract number N00173-03-1-G903.

#### References

- [1] BIERI, R. L. and GUINAN, M. W., "Grazing Incidence Metal Mirrors as the Final Elements in a Laser Driver for Inertial Confinement Fusion," *Fusion Technology* **19** (1991) 673-678.
- [2] SETHIAN, J. D., *et al.*, "Fusion Energy with Lasers, Direct Drive Targets and Dry Wall Chambers," *Nuclear Fusion* **43** (2003) 1693-1709.
- [3] McGEOCH, M., "Radio-Frequency-Preionized Xenon Z-Pinch Source for Extreme Ultraviolet Lithography," *Appl. Optics* **37**, 1651 (1998).
- [4] LATKOWSKI, J.F., ABBOTT, R.P., PAYNE, S.A., REYES, S., SCHMITT, R. C., and SPETH, J. A., "Rep-Rated X-Ray Damage and Ablation Experiments for IFE and ICF Applications," *Inertial Fusion Sciences and Applications*, Monterey, CA (2003).
- [5] OSIRIS and SOMBRERO Inertial Fusion Power Plant Designs, WJSA-92-01, DOE/ER/54100-1 Vol. 2, p. 3-11.
- [6] <http://www.srim.org/>
- [7] <http://www-ferp.ucsd.edu/ARIES/WDOCS/ARIES-IFE/SPECTRA/dd.shtml>